



PERGAMON



Atmospheric Environment 36 (2002) 1675–1689

ATMOSPHERIC
ENVIRONMENT

www.elsevier.com/locate/atmosenv

Size distribution and diurnal characteristics of particle-bound metals in source and receptor sites of the Los Angeles Basin

Manisha Singh^a, Peter A. Jaques^b, Constantinos Sioutas^{a,*}

^aDepartment of Civil and Environmental Engineering, University of Southern California, 3620 South Vermont Avenue, Los Angeles, CA 90089, USA

^bSchool of Public Health, University of California at Los Angeles, 650 Young Dr. South, Los Angeles, CA 90095, USA

Received 1 October 2001; accepted 17 January 2002

Abstract

Measurement of daily size-fractionated ambient PM₁₀ mass, metals, inorganic ions (nitrate and sulfate) and elemental and organic carbon were conducted at source (Downey) and receptor (Riverside) sites within the Los Angeles Basin. In addition to 24-h concentration measurements, the diurnal patterns of the trace element and metal content of fine (0–2.5 μm) and coarse (2.5–10 μm) PM were studied by determining coarse and fine PM metal concentrations during four time intervals of the day.

The main source of crustal metals (e.g., Al, Si, K, Ca, Fe and Ti) can be attributed to the re-suspension of dust at both source and receptor sites. All the crustals are predominantly present in supermicron particles. At Downey, potentially toxic metals (e.g., Pb, Sn, Ni, Cr, V, and Ba) are predominantly partitioned (70–85%, by mass) in the submicron particles. Pb, Sn and Ba have been traced to vehicular emissions from nearby freeways, whereas Ni and Cr have been attributed to emissions from powerplants and oil refineries upwind in Long Beach. Riverside, adjacent to Southern California deserts, exhibits coarser distributions for almost all particle-bound metals as compared to Downey. Fine PM metal concentrations in Riverside seem to be a combination of few local emissions and those transported from urban Los Angeles. The majority of metals associated with fine particles are in much lower concentrations at Riverside compared to Downey. Diurnal patterns of metals are different in coarse and fine PM modes in each location. Coarse PM metal concentration trends are governed by variations in the wind speeds in each location, whereas the diurnal trends in the fine PM metal concentrations are found to be a function both of the prevailing meteorological conditions and their upwind sources. © 2002 Elsevier Science Ltd. All rights reserved.

Keywords: Size-fractionated PM₁₀; Metals; Source site; Receptor site; Diurnal PM patterns

1. Introduction

A great number of clinical and epidemiological studies have indicated cause and effect associations between adverse respiratory effects and exposures to ambient particulate matter (PM). Epidemiological studies have shown an association between respiratory-related mortality and morbidity and levels of ambient PM with a

diameter of < 10 μm, or PM₁₀ (e.g., Adler and Fischer, 1994). From a toxicological perspective also, airborne PM has important health implications through the inhalation of PM₁₀, which can be deposited in the tracheobronchial and alveolar regions of the lung (Hileman, 1981). It is well established that these inhalable particles have higher concentrations of many potentially toxic trace elements, such as Pb, Cd, V, Fe, Zn, Cr, Ni, Mn and Cu (Natusch et al., 1974; Hlavay et al., 1992). If present in elevated concentrations in ambient air, these metals can pose an important risk to human health. The findings in a study conducted by

*Corresponding author. Tel.: +1-213-740-6134; fax: +1-213-744-1426.

E-mail address: sioutas@usc.edu (C. Sioutas).

Carter et al. (1997) demonstrate that metals may be responsible for production and release of inflammatory mediators by the respiratory tract epithelium and suggest that these mediators contribute to the toxic effects of particulate air pollutants reported in epidemiological studies. A study conducted by Ghio et al. (1999) shows that metals associated with both the water-soluble and insoluble fractions of ambient particles catalyze oxidative stress, which is a potential mechanism of tissue injury. In oil fly ash, soluble metals have been demonstrated to be responsible for oxidative stress, cell signaling, expression of inflammatory mediators, and lung injury. Particles from this specific emission are unique in their high concentrations of vanadium, nickel, and iron compounds (Kadiiska et al., 1997).

Knowledge of the size distribution of atmospheric particles within which trace elements and metals reside is not only vital in understanding PM effects on human health, but also controls the extent to which metals may be dispersed via atmospheric transport and hence is a prerequisite for the determination of rates of deposition of metals to the Earth's surface (Allen et al., 2001). Additionally, particle size distribution data is essential to assess the inhalation health hazard (Trijonis, 1983). Determination of metal levels is usually limited to estimating their quantities within total suspended particles, PM_{10} , or $PM_{2.5}$. Little work has been done to estimate the size distribution of metals in PM and relating it to health effects. Earlier efforts in this direction include a study in Spain by Espinosa et al. (2000), describing size distribution of metals in urban aerosols. Another study by Bilos et al. (1999) describes the sources, distribution, and variability of airborne trace metals in urban aerosols in Argentina. A recent study by Allen et al. (2001) reports on the size distribution of metals in atmospheric aerosols measured at rural and semi-rural locations in central England and southern Scotland. This study also attempted to explain the differing observed size distributions of a range of trace metals. However, little equivalent information is available for other areas of the world, including the Los Angeles Basin, particularly for the full aerosol size spectrum including the sub-micron fraction. Studies by Cass et al. (2000) and Hughes et al. (1998, 1999) are among the few efforts in this direction for Southern California area. Hughes et al. (1999) report on the total non-crustal PM_{10} metal content in various locations of the Los Angeles Basin, whereas studies by Cass et al. (2000) and Hughes et al. (1998) report on the concentrations of selected trace metals in ultrafine particles. However, all of these studies are based on intensive sampling campaigns ranging from a few days to a month.

In the present study we determine the size distribution as well as diurnal characteristics of particle-bound metals in two different areas that are representative of

distinct air pollution regimes in the Los Angeles Basin. The first site is a typical urban area in the vicinity of downtown Los Angeles, in which primarily vehicular, and to a lesser extent nearby industrial sources, are responsible for direct PM formation. The mobile sources are about 2–4 km upwind, and consist of two major freeways, which are frequently congested with heavy-duty diesel trucks. The second site is located in the inland valleys of the basin, about 70 km east of downtown Los Angeles, in which PM are primarily formed by secondary gas-to-particle reactions or by wind blown dust from the nearby deserts (Kim et al., 2000). PM originally emitted in urban Los Angeles is also advected in this area after several hours of suspension in the atmosphere. It is therefore common to refer to the former air pollution regime as “source” and to the latter as “receptor” areas of the Los Angeles Basin. Data in each location have been collected for a period of ≈ 5 months. As part of the work described in this paper, we also identify correlations between the concentration of trace elements and metals with similar sources of origin at these two sites.

2. Methods

2.1. Sampling locations, frequency and instrumentation

The particle-bound metal concentration measurements presented in this paper are part of the Southern California Particle Center and Supersite (SCPCS) measurement and monitoring program. In addition to the trace element and metal measurements, size-fractionated mass, inorganic ions (nitrate and sulfate), as well as elemental and organic carbon PM_{10} concentrations were measured. Two series of field experiments were conducted in two different locations of the Los Angeles Basin (Fig. 1). The first set of field tests was conducted in Downey, of central Los Angeles, whereas the second series were conducted in Riverside, CA—an inland area east of Los Angeles.

Situated near the Los Angeles “Alameda corridor”, Downey has some of the highest inhalable particle concentrations (PM_{10}) in the US, very often exceeding the National Ambient Air Quality Standard of $150 \mu\text{g m}^{-3}$. The 25-mile long Alameda corridor joins the coastal area of Long Beach, which has a large number of operational industrial plants and oil refineries, to downtown Los Angeles. The Downey site is about 10 km downwind of these refineries and about 2–4 km downwind of freeways I-710 and I-605, both of which contribute to high diesel emissions from heavy truck traffic.

The sampling location in Riverside was adjacent to the facilities of the Citrus Research Center and Agricultural Experiment Station (CRC-AES) of the

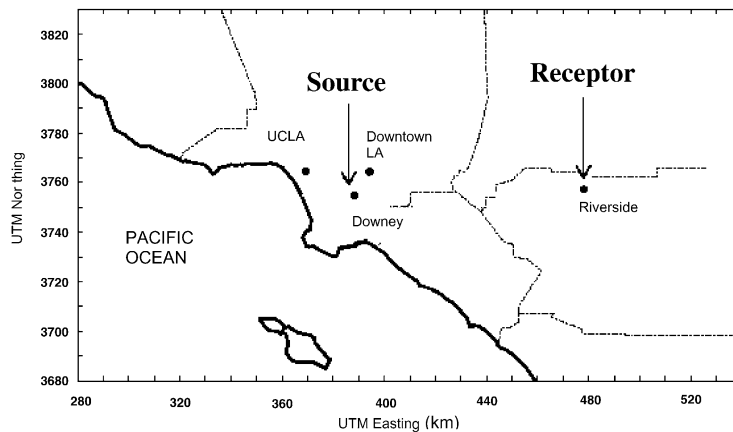


Fig. 1. Locations of source site (Downey) and receptor site (Riverside) in the Los Angeles Air Basin.

University of California, Riverside campus, ≈ 70 km directly east of downtown Los Angeles. The site is upwind of the surrounding freeways, but the area has high concentrations of ammonium nitrate due to upwind livestock and farming. Also, the aged particulate plume generated by the millions of vehicles, mostly west of downtown Los Angeles, is blown by the predominant westerly winds from Los Angeles to Riverside (Allen et al., 2000). Thus, Downey is considered a “source” site, impacted primarily by relatively fresh PM emissions, while Riverside is considered a “receptor” site, in which the aerosol consists of particles generated by secondary photochemical reactions, as well as those that reach this area, originally emitted in central Los Angeles, after aging for several hours in the atmosphere (Pandis et al., 1992).

Field tests in each location were conducted consecutively for a 5-month period. In Downey, experiments were conducted during the period of September 2000 through January 2001, whereas in Riverside field tests were conducted from February to June 2001. Size-fractionated particle samples were collected in each location by means of three collocated Microorifice Uniform Deposit Impactors (MOUDI, Model 110 MSP Corporation, Minneapolis, MN), described in more detail by Marple et al. (1991). The acceleration nozzle blocks of each MOUDI were set to rotation during field sampling in order to ensure uniform deposit of the collected particles over the substrate surface area. The MOUDIs were operated at 301 min^{-1} and configured to classify particles in the following size intervals: 0–0.10, 0.10–0.35, 0.35–1.0, 1.0–2.5 and 2.5–10 μm . The first size range (0–0.10 μm) represents the ultrafine PM mode. Several studies over the past two decades in Southern California (e.g., Hering et al., 1997; John et al., 1990) have indicated that the accumulation mode (i.e., 0.1–1 μm) may consist of two sub-modes, one peaking at

around 0.25–0.3 μm and the other at about 0.6–0.7 μm . The first mode is created by accumulation of condensable material onto primary combustion particles whereas the second mode results from accumulation of condensable material onto background sulfate particles advected into the Los Angeles Basin from out over the Pacific Ocean (Kleeman and Cass, 1998). Following the definition of Hering et al. (1997) we refer to the size range between 0.1 and 0.35 μm as the condensation sub-mode, and to the 0.35–1.0 μm size as the droplet sub-mode. The size range between 1.0 and 2.5 μm is considered a transition range between the accumulation and coarse (2.5–10 μm) PM modes.

To determine the metal and trace element content within the four larger size fractions, 47-mm Teflon filters (PTFE, Gelman, 2 μm pore, Ann Arbor, MI) were used as impaction substrates, whereas particles smaller than 0.1 μm in aerodynamic diameter were collected on a 37-mm Teflon after-filter. The Teflon filters and substrates were first weighed before and after each field tests using a Mettler 5 Microbalance (MT 5, Mettler-Toledo Inc., Highstown, NJ), under controlled relative humidity (e.g., 40–45%) and temperature (e.g., 22–24°C) conditions. At the end of each experiment, filters were stored in the control humidity and temperature room for 24 h prior to weighing in order to ensure removal of particle-bound water. Subsequent to filter weighing, the Teflon filters were analyzed by means of X-ray fluorescence in order to determine the concentrations of particle-bound trace elements and metals. The sampling protocol for size-fractionated particulate inorganic ions (i.e., sulfate and nitrate) was the same as for the metals (i.e., the same MOUDI cut-points, and the same filter substrate). The Teflon substrates were analyzed by ion chromatography to determine the concentrations of particle-bound sulfate and nitrate. A third co-located MOUDI was used to determine size-segregated PM_{10} concentrations

of organic and elemental carbon. Forty-seven millimeter aluminum-foil substrates were used for impaction of larger particles on the upper MOUDI stages, while 37-mm quartz filters (Pallflex Corp., Putnam, CT) were used as an after-filter to collect the ultrafine fraction of particles. The aluminum-foil substrates and quartz filters were analyzed by means of thermo-analysis (Fung, 1990) to determine the EC and OC content.

All three MOUDIs sampled for 24 h, starting at 6 a.m., approximately once every week during a weekday in each location. In addition to the 24-h MOUDI measurements, the diurnal patterns of trace elements and metals within the fine (0–2.5 μm) and coarse (2.5–10 μm) ambient PM fractions were determined by means of a dichotomous sampler (Partisol-Plus™, Model 2025 Sequential Air Sampler, Rupprecht and Patashnick Co. Inc., Albany, NY). PM_{2.5} and coarse particle mass and elemental composition data were provided by means of the Partisol for the following time intervals: 6 a.m.–10 a.m.; 10 a.m.–3 p.m.; 3 p.m.–8 p.m.; 8 p.m.–6 a.m. These intervals were chosen to roughly capture the morning traffic, midday and early afternoon, evening (including traffic), and overnight periods, respectively. These measurements were also conducted approximately once per week, and concurrent with the MOUDI sampling

days. Forty-seven millimeter Teflon filters were placed in the coarse and fine channels of the Partisol sampler. The mass concentration and elemental composition of fine and coarse particles were determined following the same processes described above for the 24-h MOUDI measurements. A total of 19 and 22 MOUDI measurements were made at Downey and Riverside, respectively, for determining total mass and elemental composition. Furthermore, eight 24-h Partisol measurements were made in Downey and Riverside, each consisting of four sampling periods.

3. Results and discussion

3.1. Downey data

3.1.1. PM₁₀ chemical composition, metal content and size distribution

Results of the 24-h chemical composition, by chemical group (NH₄NO₃, (NH₄)₂SO₄, EC, OC, metals and trace elements), are presented, relative to each other, as bar graphs for the five PM sub-modes studied at Downey between September 2000 and January 2001 (Fig. 2a). Over 90%, by mass, of ultrafine PM are carbonaceous,

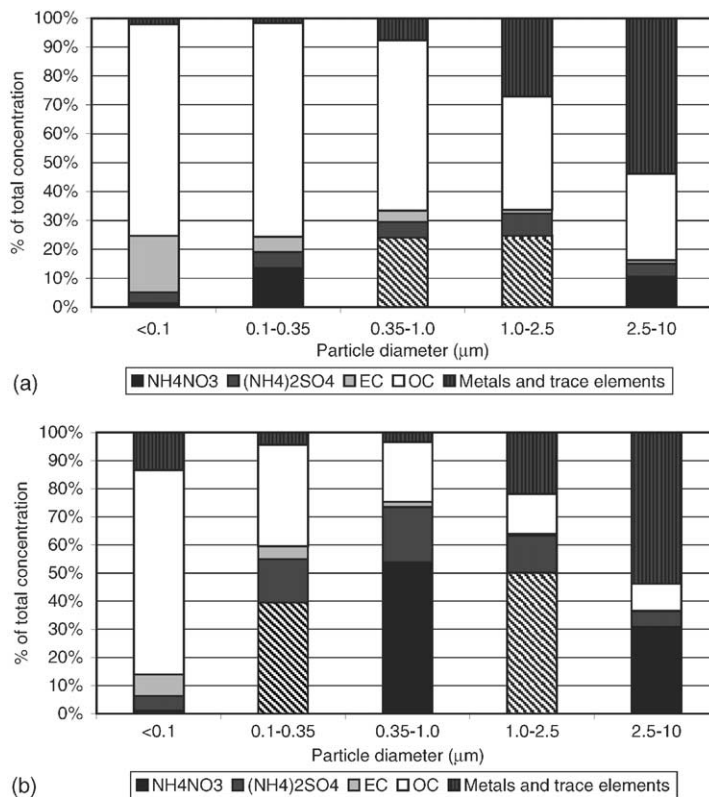


Fig. 2. Chemical mass balance of particles in five size ranges at (a) Downey and (b) Riverside.

Table 1
Limits of detection (LOD) for five PM size ranges. All values are ng m^{-3}

Metal	PM size range (μm)				
	10–2.5	2.5–1.0	1.0–0.35	0.35–0.1	<0.1
Al	0.24	0.42	0.49	0.49	0.53
Si	0.16	0.29	0.34	0.34	0.37
K	0.12	0.22	0.26	0.26	0.28
Ca	0.08	0.14	0.17	0.17	0.18
Na	0.44	0.78	0.92	0.92	0.99
Ti	0.06	0.10	0.12	0.12	0.13
V	0.04	0.07	0.08	0.08	0.09
Cr	0.04	0.07	0.08	0.08	0.09
Mn	0.07	0.12	0.14	0.14	0.15
Fe	0.05	0.10	0.11	0.11	0.12
Ni	0.04	0.06	0.07	0.07	0.08
Cu	0.04	0.06	0.07	0.07	0.08
Zn	0.04	0.07	0.08	0.08	0.09
Sn	0.57	1.01	1.18	1.18	1.28
Ba	1.75	3.14	3.69	3.69	3.48
Pb	0.16	0.29	0.34	0.34	0.37

with the average elemental and organic carbon contents being 20% and 73%, respectively. Organic carbon (74%) and nitrate (14%) are the two most prominent constituents of the condensation mode (0.1–0.35 μm). The mass fraction of nitrate increases as size increases to the droplet and transition modes. Organic carbon is still the dominant species of the droplet mode, accounting for 59% of the total measured chemical mass in that size range, whereas the nitrate content is higher (24%) compared to that found in the condensation mode. The 1–2.5 μm “intermediate” size range consists primarily of organic carbon (39% by mass), metals and elements (27%), nitrate (25%), and sulfate (8%). Finally, coarse PM consist mainly of trace elements and metals (about 54%), whereas organic carbon accounts for about 30% of coarse PM by mass.

Table 1 shows the limits of detection (LOD) values for selected metals in five PM size ranges. The different LODs for each size range reflect differences in the particulate deposit areas between MOUDI stages. In finer detail, the geometric means (and range) of the 24-h mass concentrations of selected metal and trace element species in the five PM_{10} sub-modes at Downey are presented in Table 2. Based on these values, their relative concentrations have been plotted in Fig. 3a. Crustal elements such as Al, Si, Ca and K are the most abundant metals in the coarse (2.5–10 μm) mode. The data reveal that Al, Si, K, and Ca are almost exclusively partitioned in the super micrometer size range, with about 60–80% by mass found in the coarse mode and about 15–30% of the mass concentrations in the

intermediate mode. A second group of metals (Fe and Ti) display similar size distributions, but shift with the majority (roughly 40%) of the PM mass in the “intermediate” 1–2.5 μm range and with a substantial fraction (around 30%) in the coarse PM mode. The size distributions of these two metals suggest that, although $\text{PM}_{2.5}$ is typically about 70%, or greater, of the PM_{10} fraction in Downey, resuspension of soil and road dust is a significant source of these metals.

The common origin of these metals may further be indicated by examination of the data presented in Table 4. The data clearly show a very high degree of correlation between the ambient coarse concentrations of Si and those of Ca, Ti, Mn, Fe, K and V with correlation coefficients (R^2) ranging from 0.75 to 0.98. The high degree of correlation between the metals of this group and their high relative mass (with the exception of V) in the coarse mode highly suggests that, at least, the coarse PM mode of Si, Ca, Ti, Mn, Fe, K and V originate from resuspension of soil dust.

The remaining metal elements predominate in the smaller PM modes, below 2.5 μm . About 40% of both manganese and zinc is found in the 0.35–1.0 μm range, with their remaining mass (60%) distributed relatively equally in larger and smaller particles, thereby indicating that the emission sources of these metals are split between fuel-oil combustion and soil-or-road dust resuspension. Another group of metals (Pb, Sn, Ni, Cr and V) are proportionately greater in finer particles (i.e., the accumulation mode and ultrafine fraction). Approximately 70–85% of these metals are associated with sub-micrometer particles, and over 40% of the mass concentrations of these metals are associated with particles smaller than 0.35 μm . This suggests that these species originate from anthropogenic sources, such as traffic and industrial emissions, since combustion processes contribute to the formation of small particles.

Three highly correlated groups of metals and trace elements were identified in the fine and ultrafine PM modes in Downey (Table 4). The 24-h average ambient $\text{PM}_{2.5}$ concentrations of Fe are highly correlated with those of Zn, Mn, Ti, and Pb, with R^2 varying from 0.77 to 0.80. In the fine PM mode, Fe and Ti are dominated by super micrometer particles (Fig. 3a), suggesting that soil dust resuspension may be the main source for these metals. Zn has been attributed to tire dust and municipal incineration (Cass and McRae, 1982), whereas virtually all of Pb found in the Los Angeles Basin has been attributed to vehicular emissions of mostly gasoline engines (Huntzicker et al., 1975; Lankey et al., 1998). The remarkable correlation between Pb and the rest of the three metals, despite the substantial difference in their size distributions (with Pb being partitioned in much finer particles than Fe, Ti or Zn) suggest that vehicular emissions in Downey may be indirectly responsible for the production of Fe, Zn and Ti in the

Table 2
24-h averaged mass concentrations of selected metals in five PM size ranges at Downey

Metal	PM size range (μm)				
	10–2.5	2.5–1.0	1.0–0.35	0.35–0.1	<0.1
	Geomean mass concentration (ng m^{-3}) Range (ng m^{-3})				
Al	319.84 (4945.98–2.81)	58.41 (315.52–bdl)	6.87 (87.92–bdl)	0.78 (3.02–bdl)	0.62 (1.86–bdl)
Si	346.98 (649.38–109.72)	155.28 (703.42–2.62)	45.83 (194.00–1.66)	2.54 (5.20–bdl)	9.02 (13.00–bdl)
K	100.44 (226.10–24.31)	26.87 (135.09–bdl)	34.18 (148.35–bdl)	1.00 (1.39–bdl)	0.33 (0.77–bdl)
Ca	142.28 (322.86–17.85)	75.12 (390.37–0.32)	26.59 (103.67–0.52)	0.87 (1.80–bdl)	0.40 (0.63–bdl)
Na	90.35 (237.38–26.20)	24.37 (179.89–bdl)	22.78 (54.92–bdl)	1.20 (1.93–bdl)	1.16 (2.04–bdl)
Ti	10.77 (33.53–bdl)	12.89 (52.02–bdl)	5.57 (18.07–bdl)	1.89 (7.00–bdl)	1.13 (5.46–bdl)
V	0.63 (1.70–bdl)	1.31 (3.70–bdl)	1.51 (4.97–bdl)	2.09 (6.28–bdl)	0.28 (8.92–bdl)
Cr	1.05 (14.29–bdl)	1.01 (12.00–bdl)	1.53 (7.20–bdl)	1.28 (3.47–bdl)	1.22 (19.29–bdl)
Mn	2.26 (6.48–bdl)	2.74 (10.40–bdl)	4.90 (11.70–0.41)	2.07 (3.49–0.34)	0.84 (2.81–bdl)
Fe	150.89 (477.33–0.49)	161.51 (857.14–0.22)	80.08 (224.34–1.97)	33.62 (86.39–1.36)	20.47 (93.03–7.24)
Ni	0.58 (6.30–bdl)	0.53 (5.54–bdl)	1.09 (3.80–0.17)	1.77 (6.24–bdl)	1.01 (7.70–bdl)
Cu	3.46 (8.49–bdl)	5.97 (21.65–0.20)	3.02 (8.13–bdl)	2.09 (7.79–bdl)	1.99 (11.17–0.28)
Zn	4.39 (17.11–bdl)	8.01 (28.15–bdl)	14.53 (34.44–bdl)	8.98 (22.19–bdl)	3.65 (31.09–1.13)
Sn	1.30 (3.09–bdl)	2.77 (21.39–bdl)	11.81 (76.37–bdl)	8.57 (50.78–bdl)	3.53 (16.50–bdl)
Ba	15.07 (34.43–bdl)	17.57 (70.53–bdl)	10.20 (24.61–bdl)	7.83 (9.89–bdl)	8.45 (10.68–bdl)
Pb	1.75 (4.66–0.46)	1.89 (5.1–bdl)	3.34 (7.64–bdl)	4.19 (12.65–bdl)	1.33 (7.16–bdl)

bdl denotes 'below detection limits'.

fine PM mode, in the form of resuspended road dust (including tire and paved road dust). It is also of interest to note that, historically, the ratio of the average values of iron to manganese in the South Coast of California has been found to vary from 47:1 to 53:1 (Cass and McRae, 1982; Friedlander, 1973), which is very close to the 50:1 ratio present in fine PM road dust samples (Watson, 1979). By examining the slope of the Mn–Fe regression line in Table 4, the average iron-to-manganese concentration ratio in fine PM is 55:1 (i.e., the inverse of 0.018), which is also practically identical to the previously reported values in road dust samples. This finding provides further corroboration to the argument that these metals found in fine PM in Downey originate mostly from road dust.

A high Pb–Sn as well as Pb–Ba correlation ($R^2 = 0.66$ and 0.80, respectively) within fine PM is clearly depicted in Table 4. Since Pb is originating from vehicular pollution, it can be inferred that Sn and Ba also originate from mobile sources of the nearby freeways.

Significant correlations were observed between the concentration of Ni and Cr both in the fine as well as the ultrafine modes, with R^2 of 0.54 and 0.50, respectively (Table 4). Nickel has been used as a tracer for fuel oil combustion in source-receptor modeling studies in Los Angeles (Cass and McRae, 1982). Although Cr could be emitted from diverse sources, its high correlation with Ni suggest that in Downey Cr is also emitted by the power plants and refineries of the Long Beach area that are upwind of this location.

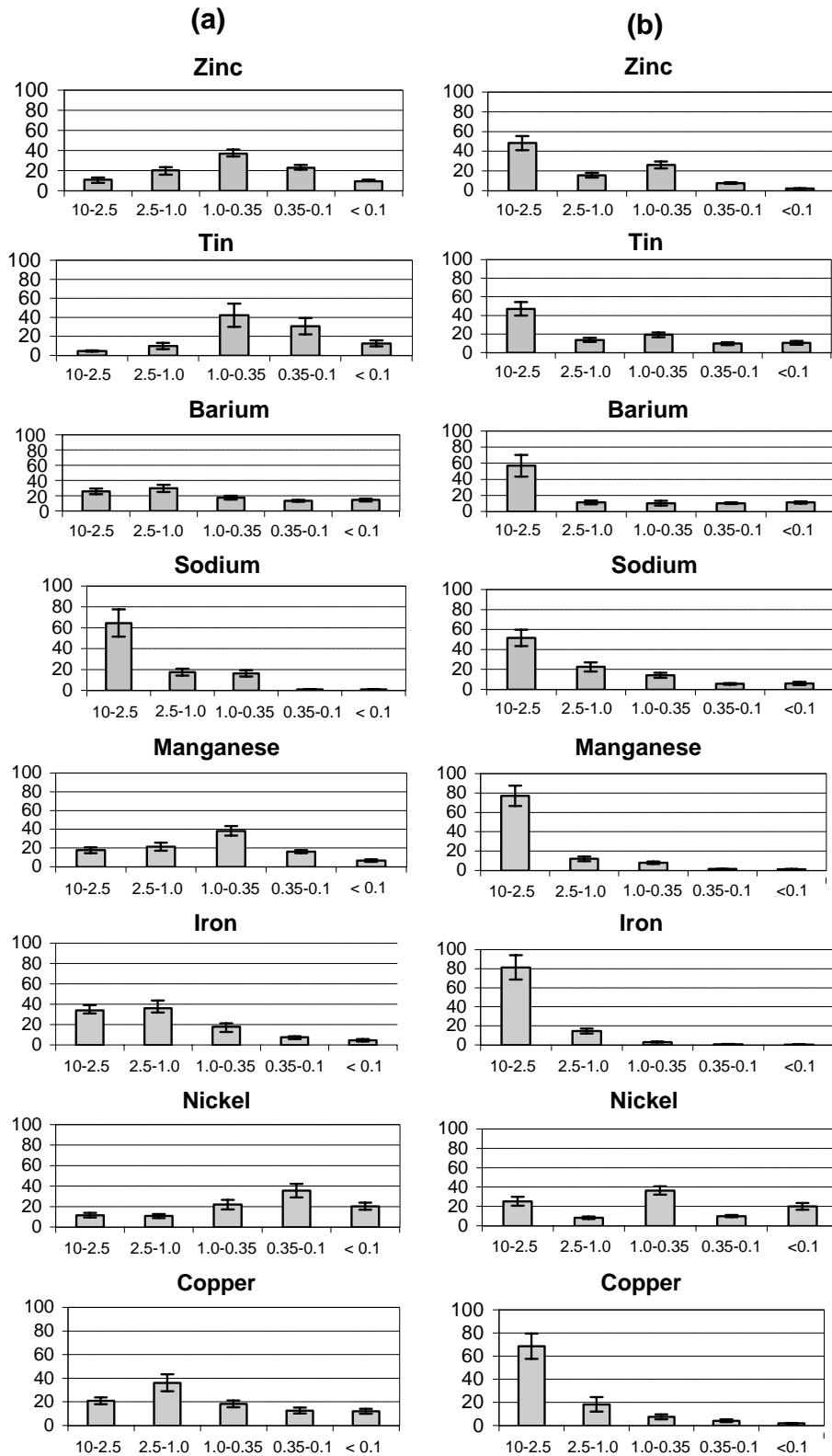


Fig. 3. Percent particle size distribution of metals at (a) Downey and (b) Riverside.

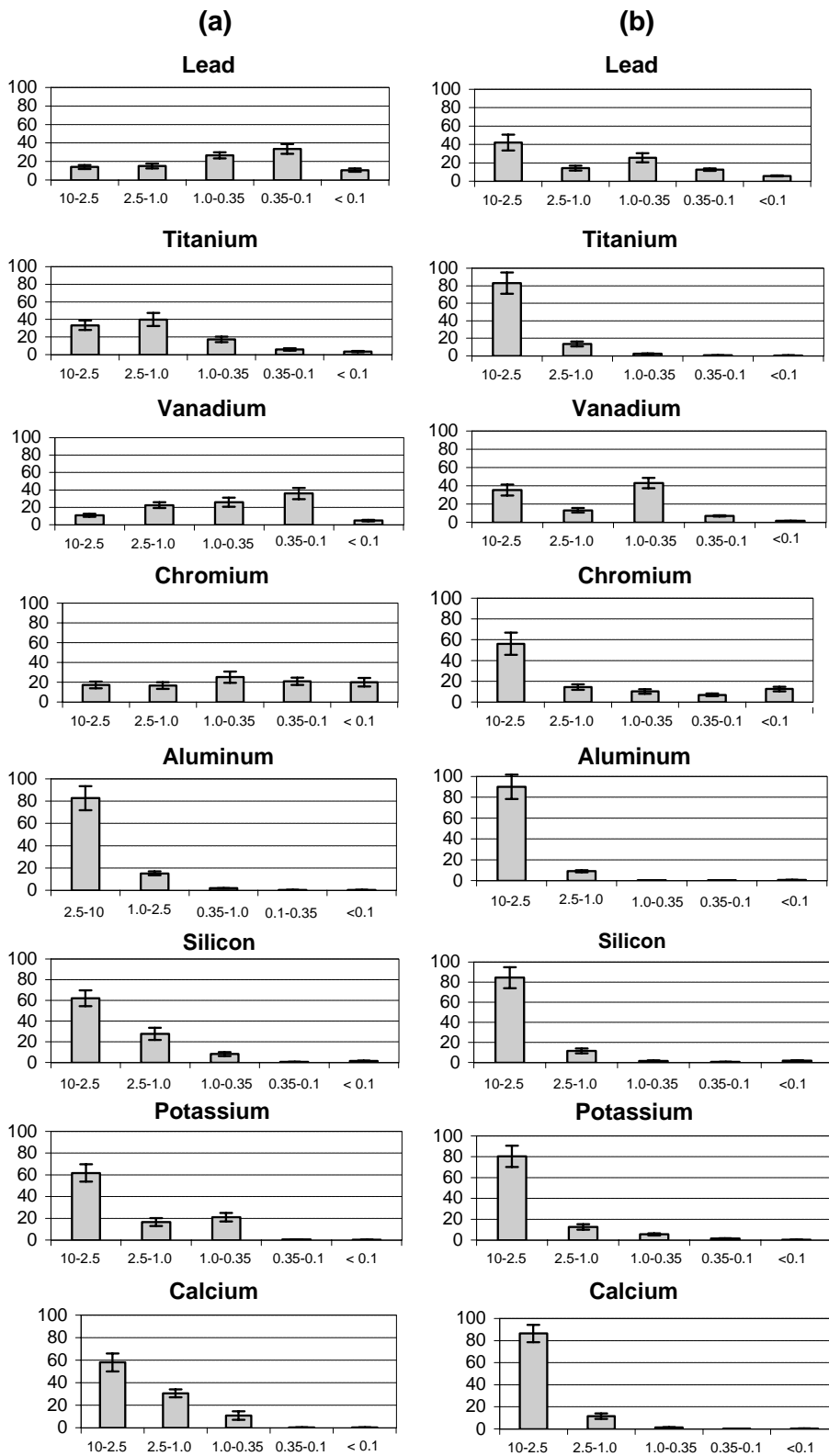


Fig. 3 (continued).

3.1.2. Diurnal patterns

Fig. 4a and b present average diurnal trends of the most predominant metals in the coarse and fine PM modes, respectively, in Downey. These measurements were conducted at Downey, between September 2000 and January 2001. The diurnal trends for each metal in the coarse PM are quite similar: the concentrations become higher in the late afternoon (between 3 and 8 p.m.); and drop sharply at night. By contrast, the metal concentrations for fine PM peak in the early morning period (6–10 a.m.) and decrease during the day. These two observations can be explained by examining the wind speed at Downey during different time periods of the day (Fig. 5a). The average wind speed is low and from the South during early morning hours. As the day progresses it shifts from the West and the velocity reaches a maximum value in the afternoon around 3 p.m. The wind speed decreases again later in the evening, shifting back to a Southerly. Coarse PM, which is primarily re-suspended by wind, is higher during the

time of day at which the wind speed is high. Fine PM metals, which mostly originate from vehicular emissions in Downey, become maximized during the early morning period when traffic peaks, and the atmospheric mixing depth and wind speed is at a minimum. The concentration of fine PM metals reaches a minimum during the afternoon period, because of the decrease in traffic, and increase in the mixing depth and wind speed, (both of which tend to disperse the vehicular emissions of the nearby freeways). Fine PM metal concentrations increase again during the nighttime, mainly due to the contributions of the evening traffic as well as the decrease in the wind speed and depression of atmospheric mixing depth.

3.2. Riverside data

3.2.1. PM₁₀ chemical composition, metal content and size distribution

Results of the 24-h chemical composition, by chemical group (NH₄NO₃, (NH₄)₂SO₄, EC, OC, metals and trace

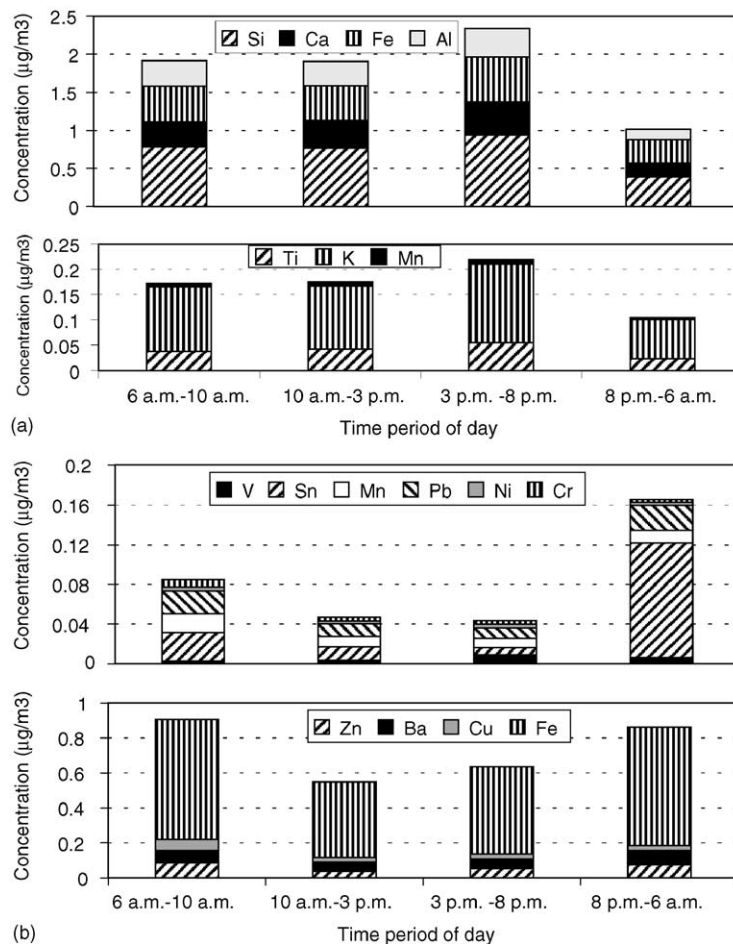


Fig. 4. Metal element concentrations as a function of time period of day in (a) coarse and (b) fine PM at Downey.

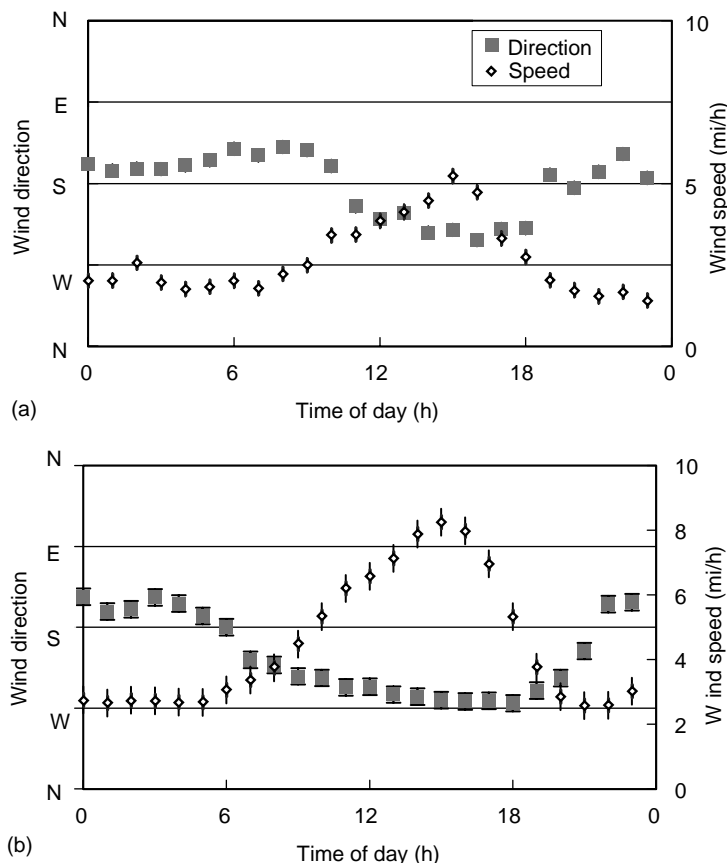


Fig. 5. Average diurnal trends of wind direction and wind speed at (a) Downey and (b) Riverside.

elements), are presented, relative to each other, as bar graphs for the five PM sub-modes studied at Riverside between February and June 2001 (Fig. 2b). As in Downey, the major constituent of ultrafine PM is carbonaceous matter (over 80% by mass), with the average elemental and organic carbon contents being 8% and 73%, respectively. Organic carbon (36%), nitrate (39%) and sulfate (16%) are the major constituents of condensation mode. The mass fraction of organic carbon decreases as PM size increases to the “droplet” and “transition” modes and is lowest (10% by mass) in the coarse mode. Over 50% of the “droplet” mode consists of nitrate with sulfate and organic carbon contributing 20% and 21% of the PM mass, respectively. Nitrate remains the major constituent of the transition mode accounting for 50% of the total PM mass, whereas sulfate and organic carbon mass fractions drop to 13% and 14%, respectively. Trace elements and metals are the second largest fraction accounting for 22% of the total PM mass in the transition mode. Finally, coarse PM consists mainly of metals and elements (53% by mass), whereas nitrate accounts for

about 31% of coarse PM mass. Unlike at Downey, nitrate constitutes an appreciable fraction of almost all PM sub-modes (except the ultrafine mode) at Riverside. In the accumulation and ultrafine modes, nitrate is mostly in the form of ammonium nitrate, and its high concentration could be attributed to the livestock and farming practices in the area of Chino, which is about 10–15 km upwind of Riverside. Previous studies have indicated that as air parcels, originating from downtown Los Angeles, are advected inland, they cross these ammonia sources (typically in early afternoon) resulting in large production of ammonium nitrate (Kleeman and Cass, 1998). By contrast, nitrate found in the coarse mode is mostly in the form of sodium nitrate, as indicated by recent studies in that area (Kim et al., 2000; Liu et al., 2000).

Following a similar trend with that in Downey, the mass fraction of metals and elements in each sub-mode decrease as particle size decreases from coarse PM to condensation sub-mode of the accumulation mode. Coarse PM has the highest percentage of metals (53% by mass) followed by the transition mode, which

consists of 22% by mass of metals and trace elements. The metal fraction decreases further in the droplet and condensation sub-modes (3% and 4% by mass, respectively) and increases to 13% in the ultrafine mode, a value which is very similar to limited data on ultrafine PM characteristics reported in an earlier study (Cass et al., 2000) conducted in the area of Riverside.

Table 3 shows the geometric mean and range of the 24-h mass concentration averages of metal and trace element species in the five PM₁₀ sub-modes at Riverside. Based on these values, the relative concentrations (as percentages of the total measured chemical mass) of these species in the five PM₁₀ sub-modes have been plotted in Fig. 3b. Unlike Downey, the mass fraction of metals found in the 2.5–10 µm range in Riverside is considerably higher than that of the 1–2.5 µm range for

most metals. The relatively coarser metal distributions at Riverside could be explained by examining the average wind speeds at the two locations. Higher wind speeds at Riverside (Fig. 5a and b) result in the re-suspension of more coarse particles. Additionally, Riverside is closer to the Southern California deserts, areas in which coarse particles account for the majority of ambient PM₁₀ (Ostro et al., 1999).

The main emission sources of crustal metals seem to be resuspension of dust at both sites. Due to higher wind speeds at Riverside, their concentrations are much higher at Riverside than in Downey (Tables 2 and 3). The data plotted in Fig. 3b reveals that in Riverside, elements like Al, Si, K, Ca, Fe, Mn and Ti are primarily present in coarse particles with percentages varying from 80% to 90%, thereby suggesting resuspension of wind-

Table 3
24-h averaged mass concentrations of selected metals in five PM size ranges at Riverside

Metal	PM size range (µm)				
	10–2.5	2.5–1.0	1.0–0.35	0.35–0.1	<0.1
	Geomean mass concentration (ng m ⁻³)				
	Range (ng m ⁻³)				
Al	550.35 (1086.59–95.81)	54.48 (185.1–8.44)	0.95 (14.92–bdl)	1.01 (505.09–bdl)	3.73 (578.24–bdl)
Si	1349.57 (2485.28–289.74)	182.42 (450–60.32)	25.71 (86.46–11.81)	10.43 (68.45–3.64)	30.48 (151.88–4.50)
K	280.37 (592.22–71.87)	43.69 (104.21–8.72)	18.95 (62.36–10.10)	4.75 (17.42–2.29)	1.01 (6.45–bdl)
Ca	644.97 (1395.20–148.59)	86.21 (191.06–29.17)	10.18 (35.14–4.01)	2.53 (9.48–0.96)	2.68 (20.59–0.50)
Na	85.26 (998.00–bdl)	37.31 (417.82–bdl)	23.63 (88.13–bdl)	9.23 (9.38–bdl)	9.96 (10.12–bdl)
Ti	62.42 (114.08–13.92)	10.16 (20.56–4.84)	1.79 (5.28–0.87)	0.40 (1.17–bdl)	0.34 (1.72–bdl)
V	2.24 (4.04–bdl)	0.83 (2.10–0.34)	2.73 (5.19–0.44)	0.45 (0.75–bdl)	0.10 (0.19–bdl)
Cr	1.15 (2.53–bdl)	0.29 (1.08–bdl)	0.21 (0.55–bdl)	0.14 (0.98–bdl)	0.26 (3.50–bdl)
Mn	12.77 (25.18–2.83)	1.99 (4.51–0.74)	1.32 (2.42–0.72)	0.24 (1.06–bdl)	0.22 (1.01–bdl)
Fe	737.55 (1385.30–157.43)	131.55 (277.78–62.22)	27.66 (64.31–15.23)	6.36 (16.38–1.61)	4.15 (23.61–0.86)
Ni	0.64 (2.03–bdl)	0.21 (1.01–bdl)	0.93 (1.94–bdl)	0.25 (0.95–bdl)	0.51 (82.69–bdl)
Cu	8.72 (13.53–3.78)	2.31 (5.93–1.21)	0.94 (5.99–0.47)	0.52 (40.00–bdl)	0.22 (4.34–bdl)
Zn	11.72 (29.01–2.43)	3.82 (10.66–1.88)	6.34 (37.92–1.81)	1.86 (39.95–0.31)	0.52 (4.94–bdl)
Sn	7.01 (30.52–bdl)	2.03 (2.97–bdl)	2.84 (6.47–bdl)	1.44 (3.53–bdl)	1.56 (3.83–bdl)
Ba	40.63 (156.22–bdl)	8.12 (16.78–bdl)	7.38 (7.50–bdl)	7.38 (7.50–bdl)	7.97 (8.09–bdl)
Pb	2.97 (4.94–bdl)	1.00 (1.61–bdl)	1.80 (3.85–bdl)	0.89 (6.58–bdl)	0.40 (1.03–bdl)

bdl denotes 'below detection limits'.

blown dust as the most significant source of these metals. This is further supported by linear regression results given in Table 4, between the concentrations of Ca, Ti, Mn, Fe, K, Al, Cu and V versus the concentration of Si in the coarse mode at Riverside. Pairing these variables in the coarse mode of PM result in very high correlation coefficients (R^2) (between 0.61 and 0.99) (Table 4). The high degree of correlation between the metals of this group reinforces the hypothesis that, at least in the coarse mode, Si, Ca, Ti, Mn, Fe, K, Al, V and Cu originate from resuspension of windblown dust from nearby deserts.

The concentrations of metals associated largely with fine particles are much lower in Riverside than in Downey (Tables 2 and 3). The only metals in Riverside having an appreciable fraction in the fine PM mode were Zn, V, Pb, Sn, Ba, Cr and Ni. Size distributions of Pb and Sn are quite similar, with more than 50% of each associated with $PM_{2.5}$ and around 40% present in

particles $<1.0\ \mu\text{m}$. Ni and V are also associated largely (75% and 65% by mass, respectively) with $PM_{2.5}$. Additionally, 66% and 52%, by mass, of Ni and V, respectively, are present in finer particles of size $<1.0\ \mu\text{m}$. It is of interest to note that the majority of these metals in the fine PM mode are mostly found in the 0.35–1.0 μm range (Fig. 3b) and not in the condensation and ultrafine modes, both of which are associated with particles originating from direct emissions. Vehicular emissions in the area of Riverside are obviously non-negligible, but are quite small compared to those generated daily by the millions of cars and diesel trucks in Los Angeles, thus their contribution to the overall fine particle mass is relatively small. Previous studies in this area have shown that fine PM in Riverside are mainly generated by secondary photochemical reactions (which would not contribute to the concentrations of metals) as well as those that reach this area, originally emitted in much higher concentrations in central Los Angeles, after aging for several hours in the atmosphere (Pandis et al., 1992; Kim et al., 2000). The high fraction of these metals in the 0.35–1.0 μm range implies that they originate from urban Los Angeles emissions, given that losses of particles in the coarse and ultrafine modes, which would have occurred during the long-range transport of these air masses eastwards, would favor this intermediate size range with increasing distances from the source. In a study conducted in the United Kingdom, Allen and colleagues (2001) similarly discussed that for some metals (e.g., Ni, Pb, and Zn) with similar size distributions, having mass median diameters of 0.5–0.6 μm , and measured in rural areas with no obvious PM sources, their high concentration was attributed to long-range transport from upwind urban areas.

Unlike metal concentrations in Downey, no significant correlations were observed between any groups of metals in the fine PM mode in Riverside, an observation that further supports the hypothesis of their long-range transport origin. As the air parcels travel eastward in the Los Angeles Basin, they pass over highly polluted areas in which a multitude of local vehicular and industrial sources contribute to the concentration of these metals. Given the variability of these sources in emission rates and diurnal trends, no significant correlation between these metals should be expected, which is consistent with our field results.

3.2.2. Diurnal patterns

The average diurnal changes in the concentrations of most predominant metals in the coarse and fine PM at Riverside are shown in Fig. 6a and b, respectively. These measurements were conducted at Riverside, between February and June 2001. The diurnal trends for each group of metals presented are quite similar within each mode. In the coarse PM, metal concentrations are

Table 4
Correlations between 24-h averaged mass concentrations of selected metals at Downey and Riverside

Site	PM mode	Metal	Metal	R^2	Slope	Intercept (ng m^{-3})	
Downey	<i>Coarse PM</i>	Si	Ca	0.97	0.47	-5.97	
		Si	Ti	0.97	0.06	-3.14	
		Si	Mn	0.98	0.01	-1.03	
		Si	Fe	0.97	0.63	5.10	
		Si	K	0.75	0.14	46.04	
		Si	V	0.77	0.001	0.37	
	<i>Fine PM</i>	Fe	Pb	0.80	0.02	4.81	
		Fe	Zn	0.79	0.06	28.36	
		Fe	Mn	0.79	0.02	4.25	
		Fe	Ti	0.77	0.05	7.76	
		Pb	Ba	0.80	3.18	8.71	
		Pb	Sn	0.66	4.58	-25.89	
	<i>Ultrafine PM</i>	Cr	Ni	0.54	0.36	3.52	
		Cr	Ni	0.50	0.37	1.26	
	Riverside	<i>Coarse PM</i>	Si	K	0.94	0.21	1.67
			Si	Ca	0.93	0.48	10.14
			Si	Ti	0.98	0.05	-0.55
			Si	Mn	0.97	0.01	-0.66
			Si	Al	0.99	0.45	-43.42
Si			Fe	0.98	0.55	-7.09	
Si			Cu	0.74	0.004	2.73	
Si			V	0.61	0.001	0.55	

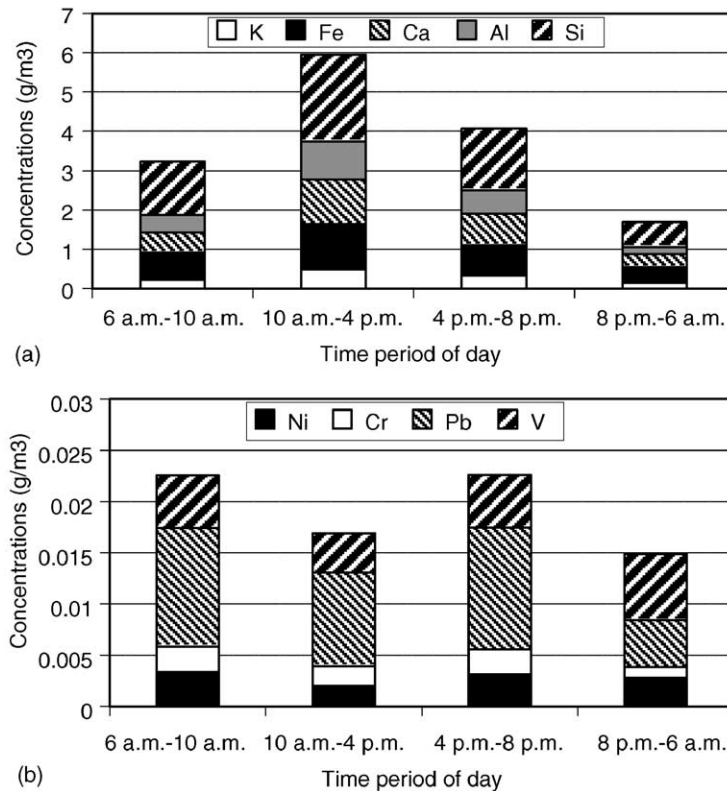


Fig. 6. Metal element concentrations as a function of time period of day in (a) coarse and (b) fine PM at Riverside.

highest in the afternoon and decrease during the evening time. Coarse PM concentrations are lowest at night and early morning periods. Similar to the coarse PM characteristics measured in Downey, the diurnal trends of metal concentrations can be explained entirely by the trends in wind speed in Riverside (Fig. 5b), given that the majority of these particles are produced by wind resuspension. The average wind speed is low during early morning and evening hours and rises as the day progresses to reach a maximum value in the afternoon around 3 p.m.

Fig. 6b shows the concentrations of selected metals in $PM_{2.5}$ as a function of time of day. Only the concentration of metals with a substantial component (i.e., over 40%) in the sub-micrometer mode, such as V, Cr, Pb and Ni were plotted. The remaining metals contain a considerable fraction of particles in the 1–2.5 μm range, which, as the data plotted in Fig. 3b indicate, represents a “tail” of the coarse PM mode, given that the fraction by mass of particles below 1 μm is <20%. Unlike Downey, the metal concentrations for fine PM in Riverside become highest during late afternoon and evening period (4–8 p.m.) and decrease substantially at nighttime. Concentrations are high again during the

morning period (6–10 a.m.) and subside during midday (10 a.m.–4 p.m.) The high relative concentrations during morning period (6–10 a.m.) are due to local background emissions, including those associated with morning traffic, coupled with the depressed atmospheric mixing depth at that time of the day. The peak in fine PM concentrations during late afternoon to early evening period (4–8 p.m.) could be attributed in part to the evening traffic, but most likely to the advection of aerosols of much higher concentrations, originally emitted by vehicular sources in urban Los Angeles. This hypothesis is further supported by the size distributions of these metals, as argued previously, which indicate partitioning in size ranges that are considerably larger to those typically associated with fresh emissions (i.e., smaller than 0.2 μm). Considering that downtown Los Angeles is about 40 miles west of Riverside, and assuming an average westerly wind speed of about 3–4 mph (Fig. 5), fine aerosols emitted mostly during the early morning traffic hours should arrive in Riverside by 4–8 p.m., which is the period during which the highest concentrations are observed. Because of the absence of any significant local sources in the vicinity, fine PM concentrations drop at night and early morning periods

in Riverside. The metal concentrations reach a minimum during midday (10 a.m.–4 p.m.), because of the increase in mixing depth as well as wind speed during that period both of which tend to disperse the particle concentrations.

4. Conclusions

The size distributions of the metals studied were influenced by a number of processes governing their concentrations in sub-micron, intermediate and coarse particles. These characteristic size distributions, combined with significant correlations within 24-h averaged concentrations of certain sub-groups of metals in coarse and fine PM modes, allow us to identify main emission sources of some of these metals. Each of the sampling sites in the Los Angeles Basin is impacted by different aerosol sources as well as formation mechanisms and thus had different ambient aerosol characteristics.

Diurnal patterns in the concentration of metals in the coarse and fine PM modes have been found to be a characteristic of fine and coarse PM sources and formation mechanisms as well as the meteorological conditions prevalent at each site.

Acknowledgements

This work was supported in part by the Southern California Particle Center and Supersite (SCPCS), funded by the US EPA under the STAR program, and the California Air Resources Board. Although the research described in this article has been funded in part by the United States Environmental Protection Agency through Grants Nos. 53-4507-0482, 53-4507-7721 and 53-4507-8360 to USC, it has not been subjected to the Agency's required peer and policy review and therefore does not necessarily reflect the views of the Agency and no official endorsement should be inferred.

References

- Adler, K.B., Fischer, B.M., 1994. Interactions between respiratory epithelial cells and cytokines: relationships to lung inflammation. *Annals of the New York Academy of Science* 725, 128–145.
- Allen, J.O., Hughes, L.S., Salmon, L.G., Mayo, P.R., Johnson, R.J., Cass, G.R., 2000. Characterization and evolution of primary and secondary aerosols during PM_{2.5} and PM₁₀ episodes in the South Coast Air Basin. Report A-22 to the Coordinating Research Council (CRC).
- Allen, A.G., Nemitz, E., Shi, J.P., Harrison, R.M., Greenwood, J.C., 2001. Size distributions of trace metals in atmospheric aerosols in the United Kingdom. *Atmospheric Environment* 35, 4581–4591.
- Bilos, C., Colombo, J.C., Skorupka, C.N., Rodriguez Pesa, M.J., 1999. Sources, distribution and variability of airborne trace metals in La Plata City area, Argentina. *Environmental Pollution* 111, 149–158.
- Carter, J.D., Ghio, A.J., Samet, J.M., Devlin, R.B., 1997. Cytokine production by human airway epithelial cells after exposure to an air pollution particle is metal-dependent. *Toxicology and Applied Pharmacology* 146, 180–188.
- Cass, G.R., McRae, G.J., 1982. Source-receptor reconciliation of South Coast Air Basin particulate air quality data. Final report to the California Air Resources Board under agreement A9-014-031, NTIS PB-82-250093.
- Cass, G.R., Hughes, L.A., Bhawe, P., Kleeman, M.J., Allen, J.O., Salmon, L.G., 2000. The chemical composition of atmospheric ultrafine particles. *Philosophical Transactions of the Royal Society of London (A)* 358, 2581–2592.
- Espinosa, A.J.F., Rodriguez, M.T., de la Rosa, F.J.B., Sanchez, J.C.J., 2000. Size distribution of metals in urban aerosols in Seville (Spain). *Atmospheric Environment* 35, 2595–2601.
- Friedlander, S.K., 1973. Chemical element balance and identification of air pollution sources. *Environmental Science and Technology* 7, 235–240.
- Fung, K., 1990. Particulate carbon speciation by MnO₂ oxidation. *Aerosol Science and Technology* 12, 122–127.
- Ghio, A.J., Stonehuerner, J., Dailey, L.A., Carter, J.D., 1999. Metals associated with both the water-soluble and insoluble fractions of an ambient air pollution particle catalyze an oxidative stress. *Inhalation Toxicology* 11, 37–49.
- Hering, S.V., Eldering, A., Seinfeld, J.H., 1997. Bimodal characteristics of accumulation mode aerosol mass distributions in Southern California. *Atmospheric Environment* 31 (1), 1–11.
- Hileman, B., 1981. Particulate matter: the inevitable variety. *Environmental Science and Technology* 15, 983–986.
- Hlavay, J., Polyak, K., Wesemann, G., 1992. Particle size distribution of minerals phases and metals in dusts collected at different workplaces. *Fresenius Journal of Analytical Chemistry* 344, 319–321.
- Hughes, L.S., Cass, G.R., Gone, J., Ames, M., Olmez, I., 1998. Physical and chemical characterization of atmospheric ultrafine particles in the Los Angeles area. *Environmental Science and Technology* 32 (9), 1153–1161.
- Hughes, L.S., Allen, J.O., Kleeman, M.J., Johnson, R.J., Cass, G.R., Gross, D.S., Gard, E.E., Galli, M.E., Morrical, B.D., Fergenson, D.P., Dienes, T., Noble, C.A., Silva, P.J., Prather, K.A., 1999. Size and composition distribution of atmospheric particles in Southern California. *Environmental Science and Technology* 33 (20), 3506–3515.
- Huntzicker, J.J., Friedlander, S.K., Davidson, C.I., 1975. Material balance for automobile emitted lead in Los Angeles Basin. *Environmental Science and Technology* 9, 448–457.
- John, W., Wall, S.M., Ondo, J.L., Winklmayr, W., 1990. Modes in the size distributions of atmospheric inorganic aerosol. *Atmospheric Environment* 22, 1627–1635.
- Kadiiska, M.B., Mason, R.P., Dreher, K.L., Costa, D.L., Ghio, A.J., 1997. In vivo evidence of free radical formation after exposure to an air pollution particle. *Chemical Research in Toxicology* 10, 1104–1108.

- Kim, B.M., Tefferra, S., Zeldin, M.D., 2000. Characteristics of $PM_{2.5}$ and PM_{10} in the South Coast Air Basin of Southern California: part I—spatial variations. *Journal of Air and Waste Management Association* 50, 2034–2044.
- Kleeman, M.J., Cass, G.R., 1998. Source contribution to the size and composition distribution of urban particulate air pollution. *Atmospheric Environment* 32, 2803–2816.
- Lankey, R.L., Davidson, C.I., McMichael, F.C., 1998. Mass balance for lead in the South Coast air Basin: an update. *Environmental Research* 78 (2), 86–93.
- Liu, D.Y., Prather, K.A., Hering, S.V., 2000. Variations in the size and chemical composition of nitrate-containing particles in Riverside, CA. *Aerosol Science and Technology* 33, 71–86.
- Marple, V.A., Rubow, K.L., Behm, S.M., 1991. A Micro Orifice Deposit Impactor (MOUDI): description, calibration and use. *Aerosol Science and Technology* 14, 434–446.
- Natusch, D.F.S., Wallace, J.R., Evans Jr., C.A., 1974. Toxic trace elements: preferential concentration in respirable particles. *Science* 183, 202–204.
- Ostro, B.D., Hurley, S., Lipsett, M.J., 1999. Air pollution and daily mortality in the Coachella Valley, California: a study of PM_{10} dominated by coarse particles. *Environmental Research* 81, 231–238.
- Pandis, S.N., Harley, R.A., Cass, G.R., Seinfeld, J.H., 1992. Secondary organic aerosol formation and transport. *Atmospheric Environment* 26 (A), 2269–2282.
- Trijonis, J., 1983. Development and application for methods for estimating inhalable and fine particle concentrations from routine hi-vol data. *Atmospheric Environment* 17 (5), 999–1008.
- Watson, Jr., J.G., 1979. Ph.D. Dissertation, Oregon Graduate Center, Beaverton, OR.